Anomalous Josephson effect controlled by an Abrikosov vortex

S. Mironov,[1] E. Goldobin,[2] D. Koelle,[2] R. Kleiner,[2] Ph. Tamarat,[3,4] B. Lounis,[3,4] and A. Buzdin[5,6]

[1]*Institute for Physics of Microstructures, Russian Academy of Sciences, 603950 Nizhny Novgorod, GSP-105, Russia*

[2]*Physikalisches Institut and Center for Collective Quantum Phenomena in LISA⁺, Universität Tübingen, Auf der Morgenstelle 14, D-72076 Tübingen, Germany*

[3]*Université de Bordeaux, LP2N, F-33405 Talence, France*

[4]*Institut d'Optique & CNRS, LP2N, F-33405 Talence, France*

[5]*University of Bordeaux, LOMA UMR-CNRS 5798, F-33405 Talence Cedex, France*

[6]*Department of Materials Science and Metallurgy, University of Cambridge, CB3 0FS, Cambridge, United Kingdom*

(Received 15 June 2017; revised manuscript received 1 November 2017; published 29 December 2017)

The possibility of a fast and precise Abrikosov vortex manipulation by a focused laser beam opens the way to create laser-driven Josephson junctions. We theoretically demonstrate that a vortex pinned in the vicinity of the Josephson junction generates an arbitrary ground state phase which can be equal not only to 0 or π but to any desired φ_0 value in between. Such φ_0 junctions have many peculiar properties and may be effectively controlled by the optically driven Abrikosov vortex. Also we theoretically show that the Josephson junction with the embedded vortex can serve as an ultrafast memory cell operating at sub THz frequencies.

DOI: 10.1103/PhysRevB.96.214515

I. INTRODUCTION

Josephson junctions (JJs) with nonzero spontaneous phase difference between the superconducting electrodes in the ground state (the so-called π, φ_0, and φ JJs) have become the subject of intensive theoretical and experimental study during the past decade [1,2]. The most striking feature of such junctions is their ability to generate a current in the superconducting circuit, thus acting as a phase battery [3–6]. In addition, relatively small variation of the system parameters may provoke dramatic changes in the ground state phase difference, which is believed to provide new effective tools for controlling the currents in microelectronic devices (see, e.g., Refs. [7,8]).

There are several generic mechanisms leading to the spontaneous appearance of nonzero Josephson phase. The basic one reveals when the superconducting (S) electrodes are separated by a ferromagnetic (F) layer. The exchange field inside the ferromagnet produces the spatial oscillations of the Cooper pair wave function, and depending on the ratio between the oscillation period and the F-layer thickness the ground state phase is equal to 0 or π (these cases are referred as 0 or π JJs, respectively) [9–11]. A peculiar situation is realized when the thickness d of the ferromagnet varies along the junction in a way that in some parts of the ferromagnet the value of d corresponds to the 0 state while in other parts to the π state (see Ref. [12] and references therein). If there is only a slight difference between the areas of the "0" and "π" regions the phase frustration can result in the appearance of a state with the spontaneous phase difference $\phi = \pm\varphi \neq 0,\pi$ which is *degenerate* (φ JJ) (see Ref. [13] and references therein). A similar effect takes place in Josephson junctions with the current injectors acting as an effective source of the phase jumps along the junction (see Refs. [14–16] and references therein). One can also obtain a φ_0 JJ, where the ground state phase $\phi = \varphi_0$ is *not degenerate*, e.g., using the JJs with broken inversion symmetry [17]. In this case the superconducting current I through the junction should not be necessarily an odd function of the phase difference ϕ and can take the form $I = I_c \sin(\phi + \varphi_0)$ [17]. Such situation is realized in the S|F|S junctions with strong spin-orbit coupling (see Refs. [17–20] and references therein) or complicated noncollinear distribution of the magnetization (see Refs. [21–23] and references therein).

However, despite the variety of opportunities for the engineering of the JJs with any desired ground state phase, it is extremely hard to tune this phase after the system is fabricated. There are just a few suggestions concerning the realization of such tuning. For example, in S|F|S junctions the transition between 0 and π states can occur by changing the temperature [10,24–26], but this transition requires the presence of magnetic impurities and very precise choice of the F-layer thickness. A more realistic situation is realized in the Josephson systems containing ballistic Bi nanowires or InSb quantum dots where the interplay between strong spin-orbit and Zeeman interactions enables the formation of π and φ_0 states, which can be tuned by an external magnetic field [18,20,27].

An alternative approach for the creation of the tunable π, $\pm\varphi$, and φ_0 JJs is based on the embedding of some intrinsic source of the current into one of the superconducting electrodes. Such current induces the nonuniform Josephson phase difference along the junction and thus modifies its ground state. The straightforward way to realize this scenario is to implant a pair of tiny current injectors serving as a source and drain [14,15,28,29]. In this case the Josephson phase along the junction reveals a jump with the amplitude determined by the value of the injected current. Recently it was demonstrated that this jump causes the appearance of the spontaneous ground state Josephson phase like in φ_0 or $\pm\varphi$ JJs depending on the parameters [16]. However, the resulting ground state appears to be very sensitive to the position of the current injectors, and thus the creation of the junction with the desired current-phase relation requires extremely precise positioning of the injectors during the fabrication process.

Interestingly, a very similar situation is realized in Josephson junctions where one of the superconducting electrodes contains Abrikosov vortices. The superconducting current circulating around the vortex core perturbs the profile of the Josephson phase and thus affects the junction ground state.

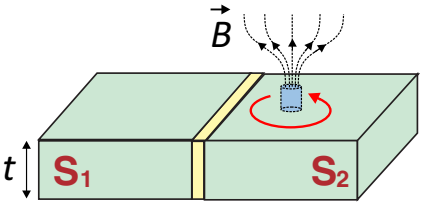

FIG. 1. Sketch of the Josephson junction with the trapped Abrikosov vortex.

The specific details of this phenomenon strongly depend on the system geometry and the orientation of the vortex.

In the simplest case of the planar JJ with the vortex trapped in one of the superconducting electrodes near the Josephson barrier, the vortex currents cross this barrier and induce the nonuniform phase profiles along the junction [30–33]. This results in the transition from the 0 to π ground state with the variation of the distance between the vortex and the Josephson barrier. Also the JJs with the embedded Abrikosov vortex are promising for the design of the cryogenic random access memory cells [34].

In the Josephson junctions of the "overlap" geometry that are formed by two thin superconducting films with the quasi-two-dimensional insulating layer in between, the cores of Abrikosov vortices tend to become oriented perpendicular to the plane of the junction. In this case the vortex currents flowing parallel to the plane of the junction induce two-dimensional phase profiles which can modify the Fraunhofer oscillations of the critical current and current-voltage characteristics, create nonquantized Josephson vortices, or even induce the nonzero ground state Josephson phase [35–41]. A similar situations is realized when such JJ is affected by the magnetic field of a small magnetic particle [42].

Recently it was experimentally demonstrated that the position of a single Abrikosov vortex can be controlled by the tip of the magnetic force microscope [43,44], the electron beam [41], the probe of the scanning tunneling microscope [45], or the focused laser beam [46]. The latter technique allows the ultrafast optically controlled positioning of an individual Abrikosov vortex which opens a new avenue for the design of novel optoelectronic superconducting devices. In particular, it becomes possible to realize the optical tuning of the current-phase relation of the Josephson junction provided the vortex is trapped in one of its superconducting leads.

In this paper we propose the concept of the optically controlled Josephson device and show that the Abrikosov vortex pinned near the JJ is a promising tool for the ultrafast tuning of the ground state phase. We consider a planar Josephson junction, see Fig. 1, with different thicknesses t of the superconducting electrodes as compared to the London penetration depth λ. We start from the limit $t \gg \lambda$. In this case depending on the vortex position the ground state phase can be equal either to 0, to π, or to any desired value in between. By moving the Abrikosov vortex, one can cause the switching between different ground states, which occurs as the type-I or type-II phase transition depending on the moving direction. Namely, by changing the distance between the vortex and the Josephson barrier one goes through the type-I transition with the jumplike changing of the ground state phase between 0 and π. At the same time, the motion of the Abrikosov vortex parallel to the junction barrier causes the type-II transition with the continuous change of the ground state phase. However, for practical applications it is more favorable to use the JJ with $t \lesssim \lambda$ which allows an easy and energy-efficient control of the vortex position due to the low vortex energy. In this case we suggest the optimal geometry for the optically driven JJ and calculate its typical working characteristics. The shifting of the vortex causes the transitions between the 0 and π states [33,47]. In this case one can use the laser to write information and realize the readout using the critical current measurements.

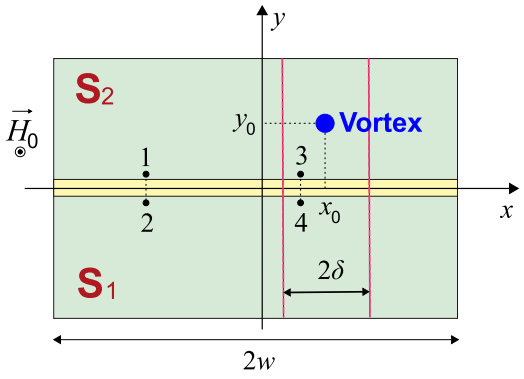

FIG. 2. The geometry of the Josephson junction under consideration.

The paper is organized as follows. In Sec. II we analyze the influence of the vortex position on the ground state of the thick planar Josephson junction and demonstrate the transition to the π and φ_0 states. In Sec. III we review the influence of the Pearl vortex on the ground state of the thin junction. In Sec. IV considering a thin junction we propose the concept of the memory cell based on the optically controlled positioning of the vortex near the JJ. In Sec. V we summarize our results.

II. TUNABLE PLANAR JOSEPHSON JUNCTION OF LARGE THICKNESS

A. Model

The system under consideration is shown in Fig. 2. The Josephson junction consists of two superconducting slabs (S_1 and S_2) of width $2w$ separated by a thin insulating (I) barrier of thickness d. We choose the origin of the Cartesian axes at the center of the insulator so that the superconductor/insulator interfaces are parallel to the xz plane and correspond to $y = \pm d/2$ while the outer boundaries of the superconductors are parallel to the yz plane and correspond to $x = \pm w$. An Abrikosov vortex is pinned inside the S_2 superconductor at the position (x_0, y_0) and its core is parallel to the z axis. Also we introduce the external magnetic field H_0 parallel to the z axis. In contrast with Refs. [33,47] we assume that the thickness h of the slabs in the z direction well exceeds the London penetration depth λ so that the boundary effects at $z = \pm h/2$ can be neglected (for simplicity we will consider an infinite sample in the z direction). We also assume that the width $2w$ of the junction satisfies the condition $\lambda \ll 2w \lesssim \lambda_J$, where λ_J is the Josephson length. Finally, we assume that $d \ll \lambda$ and neglect the variation of the magnetic field across the Josephson barrier.

If the distance y_0 between the Abrikosov vortex and the insulating layer is on the order of λ the vortex strongly modifies the properties of the Josephson junction. Indeed, in this case the superconducting current flowing around the vortex core induces a nonuniform profile of the superconducting phase along the boundary of the S_2 electrode. In Sec. II C we show that this phase can result in the appearance of the spontaneous Josephson phase across the JJ. For simplicity we assume that the vortex is situated several λ away from all outer boundaries of the superconductor. That is, its currents do not interact with them, i.e., $|x_0 \pm w| \gg \lambda$.

First we derive the analog of the Ferrell-Prange equation [48] which defines the spatial profiles of the Josephson phase $\phi(x)$ along the junction. In the S_2 superconductor the current density $\boldsymbol{j}$ is the sum of the current density $\boldsymbol{j}_{\rm sc}$, which screens the external magnetic field penetrating into the superconducting electrodes, and the vortex-induced current $\boldsymbol{j}_v$:

$$\boldsymbol{j} = \frac{1}{\mu_0\lambda^2}\left(\frac{\Phi_0}{2\pi}\nabla\theta - \boldsymbol{A}\right) = \boldsymbol{j}_{sc} + \boldsymbol{j}_v, \tag{1}$$

where $\theta(x,y)$ is the local phase of the superconducting gap function, $\boldsymbol{A}$ is the vector potential, and $\Phi_0 \approx 2.07$ fWb is the magnetic flux quantum. In the vortex-free S_1 electrode, $\boldsymbol{j}_v = 0$ and the current is determined only by the external magnetic field. Note that the expression (1) contains the terms with different length scales: the vortex current is localized at the distance $\sim\lambda$ around the vortex core while the screening currents flowing along the insulating barrier and the corresponding vector potential have a typical scale on the order of the Josephson length $\min(\lambda_J, 2w) \gg \lambda$. This allows us to realize the scale separation.

Let us consider two points 1 and 2 with the same coordinate x at the opposite superconductor/insulator interfaces with $y = \pm d/2$ (physically this means that the distance between the chosen points and the corresponding S|I interface is much smaller than λ). First, let us assume that these points lie outside the vortex neighborhood, i.e., $|x - x_0| > \delta$, where the length δ satisfies the condition $\lambda \ll \delta \ll w$ (see Fig. 2). Rewriting the projection of Eq. (1) to the x axis at $y = \pm d/2$ we find two equations

$$\frac{1}{\mu_0\lambda^2}\left(\frac{\Phi_0}{2\pi}\frac{\partial\theta^{\pm}}{\partial x} - A_x^{\pm}\right) = j_{sc,x}^{\pm}, \tag{2}$$

where the signs "±" correspond to $y = \pm d/2$. Subtracting one of these equations from another and taking into account the approximate relation $A_x^+ - A_x^- \approx H_{z0}d$ (here H_{z0} is the magnetic field inside the insulating layer) we obtain

$$\frac{1}{\mu_0\lambda^2}\left(\frac{\Phi_0}{2\pi}\frac{\partial\phi}{\partial x} + H_{z0}d\right) = j_{sc,x}^{+} - j_{sc,x}^{-}, \tag{3}$$

where $\phi(x) = \theta(x, +d/2) - \theta(x, -d/2)$ is the Josephson phase. Note that according to the Maxwell equations $j_{sc,x}^{\pm} = (1/\mu_0)(\partial H_z/\partial y)|_{y=\pm d/2}$, where $H_z(x,y)$ is the magnetic field inside the S leads [of course, $H_z(x, \pm d/2) = H_{z0}(x)$]. In the vortex-free region the magnetic field component $H_z(x,y)$ satisfies the standard London equation [49] $-\nabla^2 H_z + \lambda^{-2}H_z = 0$. Here $-\nabla^2 \equiv \partial_{xx} + \partial_{yy}$. The term $\partial_{xx}H_z \sim (\lambda/\lambda_J)^2$ and can be neglected. Hereinafter we assume that the external magnetic field H_0 is weak so that $\mu_0 H_0 \ll \Phi_0/(\lambda_J\lambda)$. In the opposite limit the variation of the magnetic field H_z along the junction scales by the length $\Phi_0/(2\mu_0 H_0\lambda)$ instead of λ_J.

The solution of the London equation inside the S_1 and S_2 electrodes allows us to calculate $\partial H_z/\partial y|_{y=\pm d/2} = -H_{z0}\,\mathrm{sgn}(y)/\lambda$ and then Eq. (3) transforms into

$$\frac{\Phi_0}{2\pi}\frac{\partial\phi}{\partial x} = -H_{z0}(d + 2\lambda). \tag{4}$$

Finally, taking the derivative of Eq. (4) over x and taking into account that $\partial H_z/\partial x = -\mu_0 j_y$ with the Josephson current density through the junction $j_y = j_c \sin\phi$ (j_c is the critical current density) we obtain the Ferrell-Prange equation in the usual form:

$$\frac{\partial^2\phi}{\partial x^2} = \frac{1}{\lambda_J^2}\sin\phi, \tag{5}$$

where

$$\lambda_J = \sqrt{\frac{\Phi_0}{2\pi\mu_0 j_c\tilde{d}}} \tag{6}$$

is the Josephson length and $\tilde{d} = (d + 2\lambda)$ is the thickness of the insulating layer renormalized by the screening currents in the superconductors.

Equation (5) should be supplemented by the appropriate boundary conditions at $x = \pm w$. Using Eq. (4) we find

$$\left.\frac{\partial\phi}{\partial x}\right|_{x=\pm w} = -\frac{2\pi\tilde{d}}{\Phi_0}H_z(\pm w). \tag{7}$$

It is important to note that the magnetic field $H_z(\pm w)$ is the sum of the external field H_0 and the field H_J induced by the Josephson current j_y flowing through the junction. It is easy to demonstrate that this self-induced field H_J has the same value and the opposite direction at the different sides of the junction. Indeed, far from the insulating layer the current flowing in the y direction is localized in the thin layers of the thickness λ near the planes $x = \pm w$ while near $y = 0$ it spreads over the whole weak link being transformed into the Josephson current. To calculate H_J it is convenient to reproduce the current distribution in the sample as the sum of the uniform current layers near $x = \pm w$ and the closed current loops localized near the insulating layer. The latter current does not contribute to H_J. Thus, the field H_J is effectively induced by two uniform current layers carrying the total current per unit length $I_y = \int_{-w}^{+w} j_y(x)dx$: $H_J(\pm w) = \mp\mu_0 I_y/2$. Of course, the derivation of this condition is based on the assumption that the system is infinite in the z direction. For the junction of a finite thickness t the coefficient in the relation $H_J(\pm w) \propto I_y$ should be calculated from the solution of the full electrodynamic problem.

Now let us analyze the behavior of the Josephson phase in the region $x_0 - \delta < x < x_0 + \delta$ near the position x_0 of the vortex. Rewriting Eq. (1) for the two points 3 and 4 inside the δ interval near the vortex (see Fig. 2) and solving the London equation for the superconducting currents we obtain the analog of Eq. (4) but with the additional vortex contribution on the right-hand side:

$$\frac{\Phi_0}{2\pi}\frac{\partial\phi}{\partial x} = -H_{z0}\tilde{d} + \mu_0\lambda^2 j_{v,x}. \tag{8}$$

Our goal is to match the solutions of Eq. (5) at different sides of this region with the boundary conditions for ϕ. First, since $\delta \gg \lambda$ the vortex current $j_{v,x}$ and the corresponding magnetic field at $x = x_0 \pm \delta$ are negligibly small. Then at $x = x_0 \pm \delta$ the magnetic field in Eq. (8) does not contain the vortex contribution and, thus, varies over distances much larger than λ so that $H_{z0}(x_0 - \delta) \approx H_{z0}(x_0 + \delta)$. Then one gets the boundary condition matching the derivatives of the Josephson phase:

$$\left.\frac{\partial\phi}{\partial x}\right|_{x_0+\delta} = \left.\frac{\partial\phi}{\partial x}\right|_{x_0-\delta}. \tag{9}$$

Second, integrating Eq. (8) over the interval $x_0 - \delta < x < x_0 + \delta$ and neglecting the term $H_{z0}\tilde{d}\delta$ since $\delta \ll w$ we find

$$\phi(x_0 + \delta) - \phi(x_0 - \delta) = \kappa, \tag{10}$$

where

$$\kappa = \frac{2\pi\mu_0\lambda^2}{\Phi_0}\int_{x_0-\delta}^{x_0+\delta} j_{v,x}^{+}dx. \tag{11}$$

Note that in Eq. (11) we may put $\delta \to \infty$ since δ is much larger than the scale of the vortex current λ. Then one sees that the phase jump κ does not depend on x_0 and is determined only by the distance y_0 between the vortex and the insulating-layer center. To calculate this phase jump let us in the first approximation neglect the small electron transparency of the insulating barrier which allows us to discard the S_1 electrode. Then the profile of the superconducting currents in S_2 can be calculated using the image technique. Note that the vortex does not create the stray magnetic field in the S_1 electrode and thus does not induce the current there. To account for the S_2 boundary, where the currents flow only in x direction, we consider a superconducting film without this boundary containing not only a vortex at (x_0, y_0) but also an antivortex at $(x_0, -y_0)$. Then we find that the supercurrent flowing at $y = +d/2$ (along the edge of the S_2 in original problem) is

$$j_{v,x}(x) = 2\frac{\Phi_0}{2\pi\mu_0\lambda^2}\frac{y_0}{r}\frac{1}{\lambda}K_1\left(\frac{r}{\lambda}\right), \tag{12}$$

where $r = \sqrt{y_0^2 + (x - x_0)^2}$ is the distance between the point $(x,0)$ at the $S_2|I$ interface and the vortex center. Substituting Eq. (12) into Eq. (11) we find

$$\kappa(y_0) = \frac{2y_0}{\lambda}\int_{-\infty}^{+\infty}\frac{1}{\sqrt{1+t^2}}K_1\left(\frac{y_0\sqrt{1+t^2}}{\lambda}\right)dt. \tag{13}$$

The resulting dependence $\kappa(y_0)$ is shown in Fig. 3. If the vortex is far from the junction ($y_0 \gtrsim 4\lambda$), then the phase jump $\kappa \to 0$. If the vortex is near the $S_2|I$ interface ($y_0 \to 0$), then $\kappa \to 2\pi$. Note that in our case the phase jump of π occurs at $y_0 \approx 0.8\lambda$, while in the case of the Pearls vortex in the ultrathin film the corresponding distance is [47] $2w \times 0.175 = 0.35w$. Note that the finite electron transparency of the insulation barrier should result in a small correction to κ on the order of $(\lambda/\lambda_J)^2$ and does not qualitatively influence further results.

Thus, the spatial profile of the Josephson phase $\phi(x)$ is determined by Eq. (5) with the boundary conditions (7)–(10). Substituting this phase profile into the expression for the

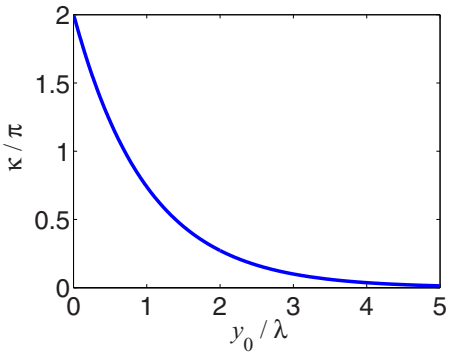

FIG. 3. The dependence of the Josephson phase jump κ on the distance y_0 between the Abrikosov vortex and the insulating layer.

Josephson current and integrating over the junction length $2w$ one obtains the current-phase relation:

$$I_y = \int_{-w}^{+w} j_c \sin[\phi(x)]dx. \tag{14}$$

In the ground state the superconducting current I_y is zero. Among the profiles $\phi(x)$ satisfying this condition the ground state corresponds to the one with the minimal free energy

$$F = \varepsilon_J\int_{-w}^{+w}\left[\frac{\lambda_J^2}{2}\left(\frac{\partial\phi}{\partial x}\right)^2 + (1 - \cos\phi)\right]dx, \tag{15}$$

where $\varepsilon_J = j_c t\Phi_0/(2\pi)$ is the Josephson energy per unit of length.

B. Asymmetric magnetic oscillations of the critical current

In this section we demonstrate that for the JJ with thick superconducting electrodes ($t \gg \lambda$) an Abrikosov vortex strongly affects the dependence of the Josephson critical current I_c on the external magnetic field H_0 producing the asymmetry of the $I_c(H_0)$ pattern with respect to $H_0 \to -H_0$. Note that previously a similar phenomenon was found for the junctions with $t \ll \lambda$ [47].

In the limit $w \ll \lambda_J$ the expression for the superconducting phase profile $\phi(x)$ along the junction can be expanded over the small parameter w/λ_J. Our strategy is to find $\phi(x)$ in the lowest approximation of the perturbation theory neglecting the corrections $\sim O(w^2/\lambda_J^2)$ which come from the phase renormalization due to the Josephson current. The resulting profile $\phi(x)$ then determines the total current I_y flowing through the junction: $I_y = j_c\int_{-w}^{+w}\sin\phi(x)dx$.

The solution of the Ferrell-Prange equation (5) satisfying the boundary conditions with the accuracy $\sim O(w/\lambda_J)$ reads

$$\phi(x) = \begin{cases}\phi_0 - \kappa/2 - h(x - x_0)/w & \text{for } x < x_0,\\ \phi_0 + \kappa/2 - h(x - x_0)/w & \text{for } x > x_0,\end{cases} \tag{16}$$

where ϕ_0 is the average phase in the vicinity of the point $x = x_0$ and $h = 2\pi\mu_0 w\tilde{d}H_0/\Phi_0$ is the dimensionless external magnetic field. Integrating the resulting Josephson current density over the width of the junction we obtain the *averaged*

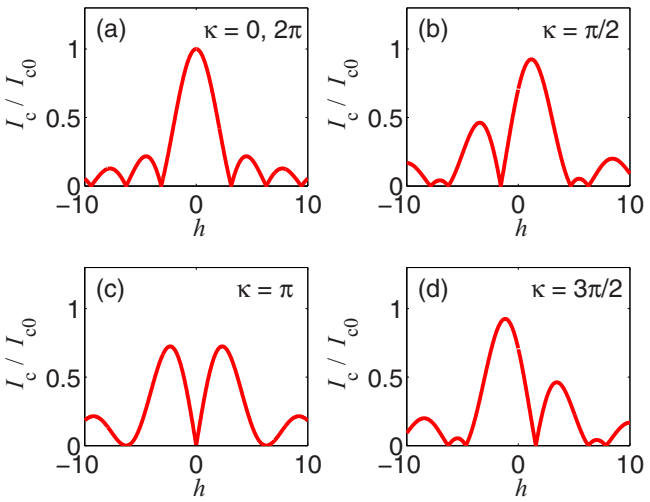

FIG. 4. Asymmetry in the Fraunhofer oscillations of the critical current in the case when the Abrikosov vortex is pinned along the line $x_0 = 0$ but at different distances y_0. The Josephson phase jump κ corresponding to y_0 is indicated in each panel.

current-phase relation $I_y(\phi_0)$:

$$I_y = \frac{I_{c0}}{h}\sin\phi_0\left[\sin\left(\frac{\kappa}{2}\right) - \cos(hX)\sin\left(\frac{\kappa}{2} - h\right)\right] - \frac{I_{c0}}{h}\cos\phi_0\sin(hX)\sin\left(\frac{\kappa}{2} - h\right), \quad (17)$$

where $X_0 = x_0/w$ and $I_{c0} = 2j_c w$. The corresponding critical current reads

$$I_c(h,\kappa,X_0) = \frac{I_{c0}}{|h|}\{1 - \cos(hX_0)\cos(h) + \cos(\kappa - h)[\cos(hX_0) - \cos(h)]\}^{1/2}. \quad (18)$$

The expression (18) clearly shows that the critical current satisfies the symmetry relations $I_c(-h,\kappa,X_0) = I_c(h,-\kappa,X_0)$ and $I_c(h,\kappa,-X_0) = I_c(h,\kappa,X_0)$. Thus, for $\kappa \neq 0,\pi$ the Fraunhofer dependencies $I_c(h)$ are asymmetric with respect to $h \to -h$. In particular, if the vortex is pinned at the central line of the junction ($X_0 = 0$) the critical current reads

$$I_c^{\rm sym}(h,\kappa,0) = I_{c0}\left|\frac{2}{h}\sin\left(\frac{h}{2}\right)\cos\left(\frac{\kappa - h}{2}\right)\right|. \quad (19)$$

The corresponding dependencies for different κ are shown in Fig. 4.

Note that at $h = 0$ the expression for the critical current reduces to $I_c^{\rm sym}(0,\kappa,0) = I_{c0}|\cos(\kappa/2)|$.

Comparing our results with the ones in Ref. [47] one sees that the asymmetry of the dependencies $I_c(H_0)$ is a generic phenomenon revealing itself for arbitrary ratios between the thickness of the superconducting electrodes t and the London penetration depth λ.

C. Phase transitions due to the shifting of the vortex

In this section we demonstrate that shifting of the Abrikosov vortex can cause phase transitions between the states with different spontaneous Josephson phase profiles. To find the profile $\phi(x)$ corresponding to the minimum of the free energy (15) we solve the Ferrell-Prange equation (5) demanding the absence of the total Josephson current (14) across the junction. For simplicity we assume that there is no external magnetic field.

To describe such phase transitions we expand the phase profile $\phi(x)$ along the junction up to the terms $\sim O(w^2/\lambda_J^2)$ accounting for the effect of the Josephson current [the higher order terms result only in small corrections to $\phi(x)$ which do not qualitatively change the picture of the phase transitions]:

$$\phi(x) = \begin{cases} \sum_{n=0}^{2} C_n^- \left(\frac{x - x_0}{\lambda_J}\right)^n & \text{for } x < x_0, \\ \sum_{n=0}^{2} C_n^+ \left(\frac{x - x_0}{\lambda_J}\right)^n & \text{for } x > x_0, \end{cases} \quad (20)$$

where the coefficients $C_0^\pm = \phi_0 \pm \kappa/2$ can be written right away, while the other $C_n^\pm$ should be determined from boundary conditions. Substituting (20) into the Ferrell-Prange equation (5), expanding the sine on the right-hand side up to $O(w^2/\lambda_J^2)$, and collecting the terms in each order of the perturbation theory separately, we find

$$C_2^\pm = \frac{1}{2}\sin\left(\phi_0 \pm \frac{\kappa}{2}\right). \quad (21)$$

The boundary conditions (7)–(9) give the other two equations:

$$C_1^- = C_1^+, \quad (22)$$

$$C_1^- - 2C_2^-\frac{w + x_0}{\lambda_J} = -C_1^+ - 2C_2^+\frac{w - x_0}{\lambda_J}. \quad (23)$$

Writing Eq. (23) we take into account that in the absence of the external magnetic field $H_z(+w) = -H_z(-w)$. Obviously in the ground state both $H_z(\pm w) = 0$ due to the absence of the current through the junction. Thus,

$$C_1^\pm = \frac{x_0}{\lambda_J}\sin\phi_0\cos\left(\frac{\kappa}{2}\right) - \frac{w}{\lambda_J}\cos\phi_0\sin\left(\frac{\kappa}{2}\right). \quad (24)$$

The expressions (21) and (24) define the Josephson phase profile $\phi(x)$ which now depends only on ϕ_0. To find ϕ_0 we take into account that in the ground state the total Josephson current $I_y = 0$. Substituting $\phi(x)$ into Eq. (14) with $I_y = 0$ we obtain the following equation:

$$\cos\left(\frac{\kappa}{2}\right)\sin\phi_0 - X_0\sin\left(\frac{\kappa}{2}\right)\cos\phi_0 + \frac{w^2}{12\lambda_J^2}\left\{\left[\left(1 - 3X_0^2\right) + \left(1 + 3X_0^2\right)\sin^2\left(\frac{\kappa}{2}\right)\right]\sin(2\phi_0) + X_0\sin\kappa\left[\left(3 + X_0^2\right)\cos^2\phi_0 - 2X_0^2\right]\right\} = 0, \quad (25)$$

where again we have introduced the dimensionless parameter $X_0 = x_0/w$.

The free energy is

$$F(\phi_0) = F_0 + 2w\varepsilon_J f(\phi_0), \quad (26)$$

where F_0 does not depend on the phase ϕ_0, and the dimensionless function $f(\phi_0)$ is

$$f(\phi_0) = -\cos\phi_0\cos\left(\frac{\kappa}{2}\right) - X\sin\phi_0\sin\left(\frac{\kappa}{2}\right) + \frac{w^2}{24\lambda_J^2} \times [2X^3\sin(2\phi_0)\sin\kappa - 3(1 - X^2)\cos(2\phi_0) - (1 - 3X^2)\cos(2\phi_0)\cos\kappa]. \quad (27)$$

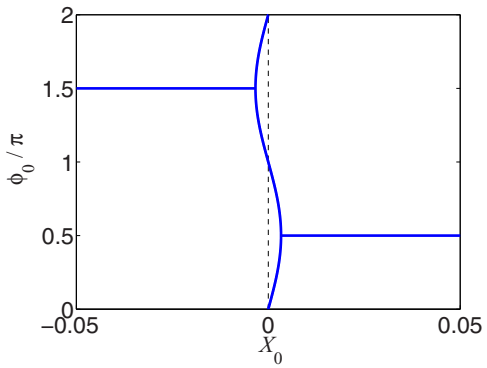

FIG. 5. The dependence of the equilibrium Josephson phase ϕ_0 on the vortex position X_0 near the phase transition. The distance between the vortex and the junction is chosen in a way that the phase jump $\kappa = \pi$. The junction width is $w = 0.1\lambda_J$.

Before proceeding with the general analysis of Eqs. (25) and (26) let us consider two limiting cases (i) $X_0 = 0$ and (ii) $\kappa = \pi$ illustrating the general features of the Josephson phase behavior.

1. Phase jump equal to π

When the Abrikosov vortex produces the phase jump $\kappa = \pi$ (i.e., $y_0 \approx 0.8\lambda$) the situation formally coincides with the one for the S|F|S junction with the steplike thickness of the F layer [12]. In this case Eq. (25) for the phase ϕ_0 transforms into

$$-X_0 \cos\phi_0 + \frac{w^2}{6\lambda_J^2}\sin(2\phi_0) = 0. \tag{28}$$

For $|X_0| > w^2/3\lambda_J^2$ this equation has the series of solutions $\phi_0 = \pm\pi/2 + 2\pi n$ (n is an integer number) while in the narrow region $|X_0| < w^2/3\lambda_J^2$ the additional solutions exist: $\phi_0 = \alpha + 2\pi n$ and $\phi_0 = \pi - \alpha + 2\pi n$ with $\alpha = \arcsin(3X_0\lambda_J^2/w^2)$.

The function $f(\phi_0)$ which defines the free energy (26) takes the form

$$f(\phi_0) = -X_0 \sin\phi_0 - \frac{w^2}{12\lambda_J^2}\cos(2\phi_0). \tag{29}$$

One can check that $f(\pm\pi/2) = \mp X_0 + w^2/12\lambda_J^2$ and $f(\alpha) = f(\pi - \alpha) = -3X_0^2\lambda_J^2/2w^2 - w^2/12\lambda_J^2$. Thus, in the region $|X_0| > w^2/3\lambda_J^2$ the equilibrium phase is $\phi_0 = (\pi/2)\mathrm{sgn}(X_0) + 2\pi n$ while for $|X_0| < w^2/3\lambda_J^2$ the minimum of the free energy corresponds to the degenerated states $\phi_0 = \alpha + 2\pi n$ and $\phi_0 = \pi - \alpha + 2\pi n$. The dependencies $\phi_0(X_0)$ near the transition point are shown in Fig. 5. For convenience for each phase we choose n in a way that $0 < \phi_0 < 2\pi$.

Clearly, the vortex motion along the junction results in the series of two type-II phase transitions at $X_0 = \pm w^2/3\lambda_J^2$ with continuously changing ϕ_0 and the jump in the second derivative of the free energy over X_0. This situation is very similar to the formation of the ϕ JJ in the stacked S|F|S systems [13]. However, in contrast with the S|F|S JJs, the Abrikosov vortex enables the real-time tuning of the equilibrium phase.

2. Vortex at the central line of the junction

Now let us turn to the limiting case when the Abrikosov vortex is placed at the central line of the junction where $X_0 = 0$. In this case Eq. (25) takes the form

$$\cos\left(\frac{\kappa}{2}\right)\sin\phi_0 + \frac{w^2}{24\lambda_J^2}(3 - \cos\kappa)\sin(2\phi_0) = 0. \tag{30}$$

The number of the solutions depends on the phase jump κ. For $|\kappa - \pi| > 2w^2/3\lambda_J^2$ there are only two series of the solutions $\phi_0 = 0 + 2\pi n$ and $\phi_0 = \pi + 2\pi n$ while for $|\kappa - \pi| < 2w^2/3\lambda_J^2$ two additional series $\phi_0 = \pm\beta + 2\pi n$ appear, where

$$\beta = \arccos\left[-\frac{12\lambda_J^2}{w^2}\frac{\cos\left(\frac{\kappa}{2}\right)}{(3 - \cos\kappa)}\right]. \tag{31}$$

To simplify this expression it is convenient to introduce the deviation $\delta\kappa$ of the phase jump from π: $\kappa = \pi + \delta\kappa$. Since $|\delta\kappa| \ll 1$ one obtains $\beta \approx \arccos[(3\lambda_J^2/2w^2)\delta\kappa]$.

The function $f(\phi_0)$ which defines the system free energy [see Eq. (27)] is

$$f(\phi_0) = \cos\phi_0 \sin\left(\frac{\delta\kappa}{2}\right) - \frac{w^2}{24\lambda_J^2}(3 - \cos\delta\kappa)\cos(2\phi_0). \tag{32}$$

Expanding Eq. (32) over $\delta\kappa$ up to $O(\delta\kappa^2)$ and at the same time neglecting the terms $\sim O(w/\lambda_J)^4$ we find

$$f(0) = \frac{\delta\kappa}{2} - \frac{w^2}{12\lambda_J^2}, \quad f(\pi) = -\frac{\delta\kappa}{2} - \frac{w^2}{12\lambda_J^2}, \tag{33}$$

$$f(\pm\beta) = \frac{3\lambda_J^2}{8w^2}\delta\kappa^2 + \frac{w^2}{12\lambda_J^2}. \tag{34}$$

Thus, the ground state phase is $\phi_0 = 0 + 2\pi n$ for $\kappa < \pi$ and $\phi_0 = \pi + 2\pi n$ for $\kappa > \pi$ while the states with $\phi_0 = \pm\beta + 2\pi n$ are not favorable at any phase jumps κ. As a result, the vortex motion along the central line of the junction (with $X = 0$) causes the type-I phase transition accompanied by the discontinuous changing of the $\phi(x)$ profile and the jump in the first derivative of the free energy over $\delta\kappa$ [see Eq. (33)].

3. Arbitrary position of the vortex

In Secs. II C 2 and II C 3 it is shown that the type of the phase transition provoked by the vortex motion strongly depends on the direction of this motion. Here we analyze the general case of the arbitrary position of the vortex. To do this we numerically find all solutions of Eq. (25) and then choose the one which corresponds to the minimal energy (26). The results are presented in Figs. 6 and 7. Interestingly, the behavior of the value of ϕ_0 in the ground state for different parameters X_0 and κ is well reproduced by the simple estimate presented below.

One can check that since $|X_0| \leqslant 1$ the expression inside the braces in Eq. (25) clearly satisfies the inequality $|\{\ldots\}| \leqslant 12$. Thus, outside the narrow parameter region defined by the two simultaneous conditions $|X_0| < w^2/\lambda_J^2$ and $|\kappa - \pi| < w^2/\lambda_J^2$ the terms $\propto w^2/\lambda_J^2$ in Eq. (25) are not sufficient and can be neglected. Then in the ground state the phase ϕ_0 takes the value

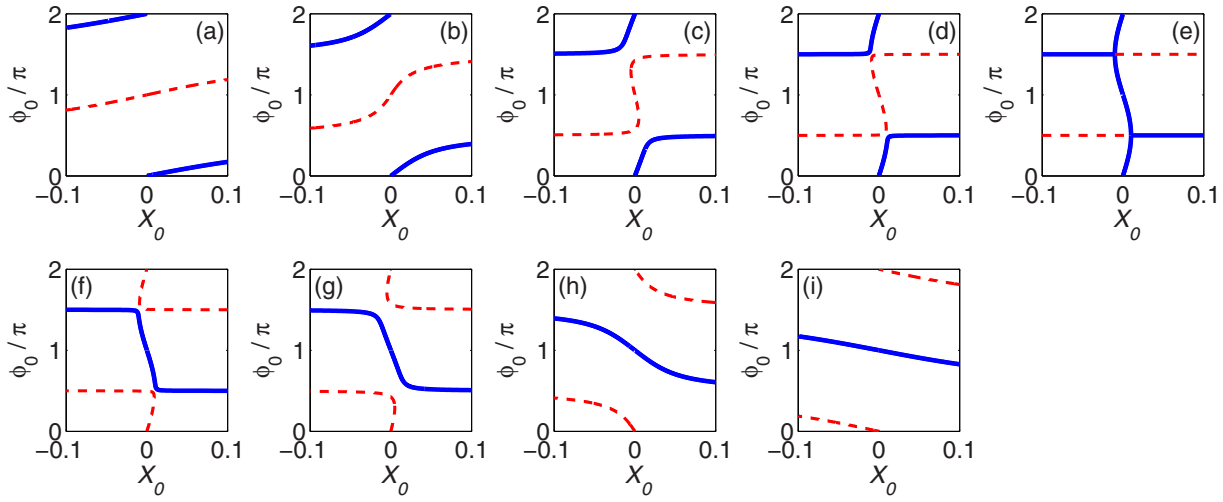

FIG. 6. The dependencies of the ground state phase ϕ_0 on the dimensionless vortex position X_0 along the junction for different values of the phase jump κ. The value $\delta\kappa/\pi = (\kappa - \pi)/\pi$ is equal to (a) -0.02; (b) -0.01; (c) -0.0015; (d) -0.0001; (e) 0; (f) 0.0001; (g) 0.0015; (h) 0.01; (i) 0.02. The blue solid lines correspond to the stable branches realizing the minima of the free energy while the red dashed curves show the metastable solutions for ϕ_0.

$\phi_0 = \tilde{\phi}_0$, where $\sin\tilde{\phi}_0 = \rho^{-1} X_0 \sin(\frac{\kappa}{2})$, $\cos\tilde{\phi}_0 = \rho^{-1}\cos(\frac{\kappa}{2})$, $\rho = \sqrt{\cos^2(\frac{\kappa}{2}) + X_0^2 \sin^2(\frac{\kappa}{2})}$.

In contrast, for $|X_0| < w^2/\lambda_J^2$ and $|\kappa - \pi| < w^2/\lambda_J^2$ the situation is more rich. In this parameter region we can expand Eq. (25) up to the terms $\sim O(w^2/\lambda_J^2)$. Then one obtains the equation

$$-\frac{\delta\kappa}{2}\sin\phi_0 - X_0\cos\phi_0 + \frac{w^2}{6\lambda_J^2}\sin(2\phi_0) = 0, \qquad (35)$$

where $\delta\kappa = \kappa - \pi$.

First let us analyze the dependencies of the value of ϕ_0 in the ground state as a function of X_0 for different $\delta\kappa \neq 0$. Depending on X_0, Eq. (35) has two or four solutions for ϕ_0. To classify these solutions it is convenient to consider the function $X_0(\phi_0) = \frac{w^2}{3\lambda_J^2}\sin\phi_0 - \frac{\delta\kappa}{2}\tan\phi_0$ which is uniquely defined. The numerical analysis shows that the minimum of the free energy for the fixed X_0 corresponds to the monotonic branch $X_0(\phi_0)$ at the interval $\pi/2 < \phi_0 < 3\pi/2$ for $\delta\kappa > 0$ or at the union of the intervals $3\pi/2 < \phi_0 < 2\pi$ and $0 < \phi_0 < \pi/2$. Also for each sign of $\delta\kappa$ there is another branch of the function $X_0(\phi_0)$ which determines one metastable ϕ_0 for the fixed X_0 in the case $|\delta\kappa| > 2w^2/3\lambda_J^2$ and three metastable solutions in the case $|\delta\kappa| < 2w^2/3\lambda_J^2$ (see Fig. 6). Note that in the ground state the dependencies of ϕ_0 and the free energy on X_0 are continuous which indicates the absence of the phase transitions for $\delta\kappa \neq 0$.

In contrast, the dependencies $\phi_0(\delta\kappa)$ for the fixed X_0 demonstrate the type-I phase transition in the case when $|X_0| < w^2/2\lambda_J^2$. Indeed, Eq. (35) can be rewritten in the form $\delta\kappa = \frac{2w^2}{3\lambda_J^2}\cos\phi_0 - 2X_0\cot\phi_0$. The values ϕ_0 corresponding to the energy minimum belong to the interval $0 < \phi_0 < \pi$

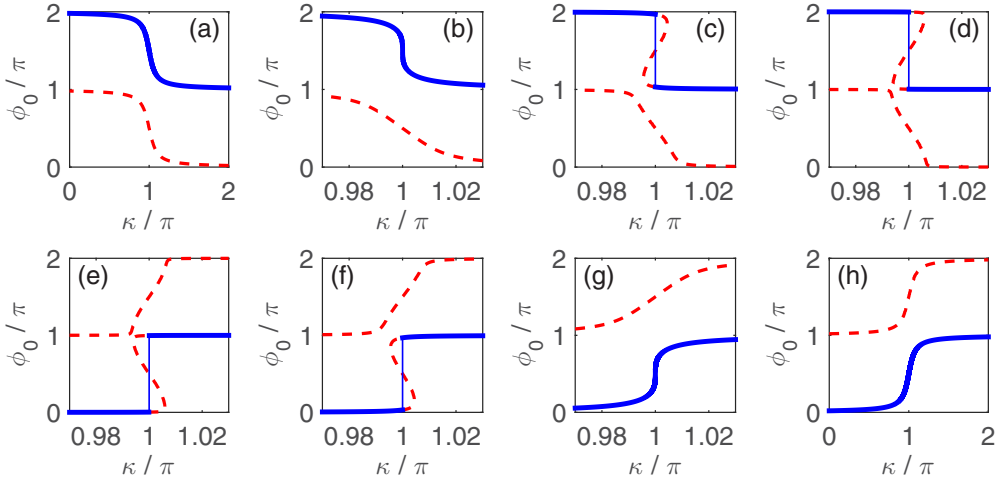

FIG. 7. The dependencies of the ground state phase ϕ_0 on the phase jump κ for different values of the vortex position X_0. The value X_0 is equal to (a) -10^{-1}; (b) -10^{-2}; (c) -10^{-3}; (d) -10^{-4}; (e) 10^{-4}; (f) 10^{-3}; (g) 10^{-2}; (h) 10^{-1}. The blue solid lines correspond to the stable branches realizing the minima of the free energy while the red dashed curves show the metastable solutions for ϕ_0.

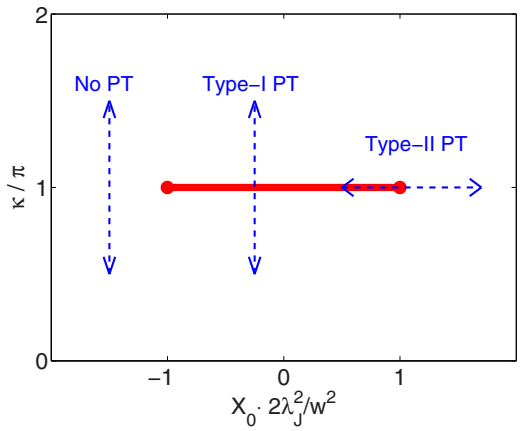

FIG. 8. The X_0-κ diagram showing the line of the type-I phase transition ending with two critical points (red straight curve). The blue dashed curves show the possible trajectories of the Abrikosov vortices corresponding to different type of the phase transitions (PT).

for $X_0 > 0$ and $\pi < \phi_0 < 2\pi$ for $X_0 < 0$. For $|X_0| > w^2/2\lambda_J^2$ the stable branch of the function $\delta\kappa(\phi_0)$ is monotonic, and thus the inverse dependence of the ground state phase ϕ_0 vs $\delta\kappa$ is uniquely defined. However for $|X_0| < w^2/2\lambda_J^2$ the function $\delta\kappa(\phi_0)$ becomes nonmonotonic and the ground state phase reveals a jump at $\delta\kappa = 0$ indicating the type-I phase transition (see Fig. 7).

Thus, on the parameter plane X_0-κ there is the segment $|X_0| < w^2/2\lambda_J^2$ at the line $\kappa = \pi$ separating the phases with different ϕ_0 in the ground state corresponding to the points of the type-I phase transition (see Fig. 8). The ends of this segment are the critical points. Thus, the vortex motion along the plane of the Josephson junction can cause either the jump of the ground state phase ϕ_0 or the continuous changing of ϕ_0 depending on whether the vortex crosses the segment corresponding to the phase transition or not.

Note that the requirement $t \gg \lambda$ which was assumed throughout this section permits us to obtain the full analytical solution. However, qualitatively the formation of ϕ_0 junctions should remain possible also in the intermediate regime $t \sim \lambda$ which is realized in typical experiments on the optical manipulation of vortices [46].

III. THIN PLANAR JOSEPHSON JUNCTION

The rich variety of possible phase transitions discussed in Sec. II opens a way for the optical sculpturing of the ground state of the JJ by performing controllable jumps of the vortex between several points. However, in such experiments the absorbed laser power needed for one jump can be substantially decreased by making the thickness of the superconducting electrodes on the order of λ or even less. In this case the description of the nonlinear phenomena responsible for the emergence of the φ_0 state requires sophisticated numerical calculations which are on the way and will be published elsewhere. In Sec. IV we will focus on the linear phenomena which allow the realization of promising devices for the superconducting electronics based on the JJ with $t \lesssim \lambda$. To simplify the calculations we will restrict ourselves for the limit $t \ll \lambda$ keeping in mind that the obtained results should qualitatively remain valid also in the intermediate regime $t \lesssim \lambda$. If the thickness $t \ll \lambda$, then the effective vortex size is $\lambda_P = \lambda^2/t$—the so-called Pearl length. The extreme case when $\lambda_P > 2w$ was studied in several works [33,47,50,51] and allows for the analytical solution. Therefore we do not rederive these case here, but rather review the key results in this section.

The phase distribution induced by a single vortex was derived in Refs. [33,47,50]. The phase induced by the vortex along the JJ length is given by [50] (in our notations)

$$\phi(x) = -2\arctan\frac{-\sin\left(\frac{\pi x}{2w}\right) + \cosh\left(\frac{\pi y_0}{2w}\right)\sin\left(\frac{\pi x_0}{2w}\right)}{\sinh\left(\frac{\pi y_0}{2w}\right)\cos\left(\frac{\pi x_0}{2w}\right)}. \tag{36}$$

It turns out that the vortex close to the JJ induces almost a steplike phase profile, with the step height (discontinuity of the Josephson phase) approaching 2π when $y_0 \to 0$. As y_0 increases, the steplike profile of the induced phase smears. At the distances $y_0 \gtrsim 2w$ the vortex induces just a constant (x independent) phase at the junction, which, however, depends on x_0, namely [50] $\phi = \pi x_0/w$. By changing the vortex coordinates (x_0, y_0), one can provoke the transitions between different junction ground states.

Further, the effect of the vortex (induced phase) on the critical current pattern $I_c(H)$ was calculated [47]. It was found that the vortex situated along the symmetry line $x_0 = 0$ may result in vanishing $I_c(0)$ if $y_0 \approx 0.350w$. This effect is similar to zero $I_c(0)$ in the 0-π JJ; however the phase profile is different from steplike. It is important to mention that y_0 corresponding to $I_c(0) = 0$ is on the order of w in the case of a thin film, and $y_0 \sim \lambda$ in the case of a thick film. Thus, it is much easier to control the JJ by moving the vortex in the thin film.

IV. OPTICALLY CONTROLLED 0-π TRANSITIONS IN THIN PLANAR JOSEPHSON JUNCTIONS

In this section we propose the concept of an optoelectronic superconducting device which exploits the possibility to realize the ultrafast switching of the critical current of the Josephson junction by the controllable displacement of the vortex. We consider the system shown in Fig. 9. The planar Josephson junction of the thickness $t \ll \lambda$ is embedded into a superconducting strip. The length $2w$ of the junction is assumed to be smaller or on the order of the effective Pearl length $\lambda_P = \lambda^2/t$ [52,53]. Previously, it was shown that in this case the vortex trapped inside the superconducting lead strongly influences the critical Josephson current I_c [32,33]. Specifically, the shifting of the vortex along the central line of the strip (the y axis) at the distances of the order of w away from the junction results in the 0-π transition which is revealed through the vanishing of I_c.

The strong sensitivity of I_c to the vortex position allows us to use an optically controlled Josephson junction as an ultrafast optoelectronic superconducting memory cell where the information is stored by the vortex position. Specifically, the switching between the states "0" and "1" can be realized as the vortex displacement between two artificial pinning

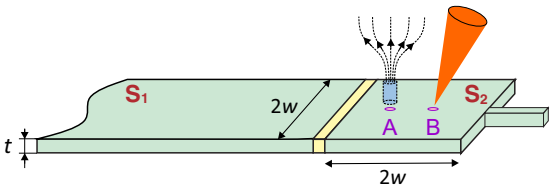

FIG. 9. The sketch of the Josephson junction which enables optical switching of the critical current by the controllable vortex displacement. The S_2 lead has the form of the square of the size $2w \times 2w$ and contains two artificial defects A and B which can efficiently trap the vortex. The laser beam focused at the nonoccupied pinning center creates an attractive thermal force acting on the vortex and provokes the jump of the vortex from one pinning center to another.

centers A and B created at the central line (y axis) of the junction. Keeping in mind the technique demonstrated in Ref. [46] we may suggest realizing the writing operation by applying the focused laser beam to the point which corresponds to the desired vortex position. At the same time, the readout can be performed by measuring the voltage on the junction at the fixed current. Indeed, the critical current I_c depends on whether the vortex is pinning at the center A or B so that $I_c^A \neq I_c^B$ (for distinctness we suppose that $I_c^B > I_c^A$). So if the JJ is a part of the electrical circuit maintaining the constant current with $I_c^A < I < I_c^B$ then the vortex skip from the point B to the point A will produce the transition from the zero voltage state ($I < I_c^B$ and the JJ has zero resistance) to the finite voltage state ($I > I_c^A$ and the resistance is finite).

In what follows we estimate the optimal characteristics of the described memory cell and highlight the main physical factors which have a strong influence on its working regimes. The position and strength of the pinning centers and the geometry of the superconducting leads should be chosen in a way which allows us to perform guaranteed laser-controlled switching between the states with the maximal frequency.

The most important factor affecting the properties of the suggested device is the pinning force F_p trapping the vortex near the pinning center. In order to stabilize the vortex position the vortex pinning should be large enough but not too strong to permit an easy vortex manipulation by a laser beam. The lower threshold for the pinning force is determined by the vortex attraction to the sample boundaries. If the pinning centers are placed at the central line of the junction the attraction forces to the opposite slab boundaries are nearly compensated in contrast with the attraction to the insulating layer. The best way to minimize this attraction seems to be to choose the S_2 electrode in the form of the square with the side $w \sim \lambda_P$ and fabricate the pinning cites near its center.

Let us calculate the force $F_{\text{att}}(y)$ attracting the vortex to the square boundaries as a function of the vortex displacement y_v from the insulating layer assuming zero displacement from the junction central line in the direction perpendicular to the y axis (in this case the force $\mathbf{F}_{\text{att}}$ is also directed along the y axis). To do this we need to solve the London equation for the magnetic field H_z induced by the vortex currents with the boundary conditions requiring the absence of the normal component of the current at the S_2-electrode edges. Then the projection of

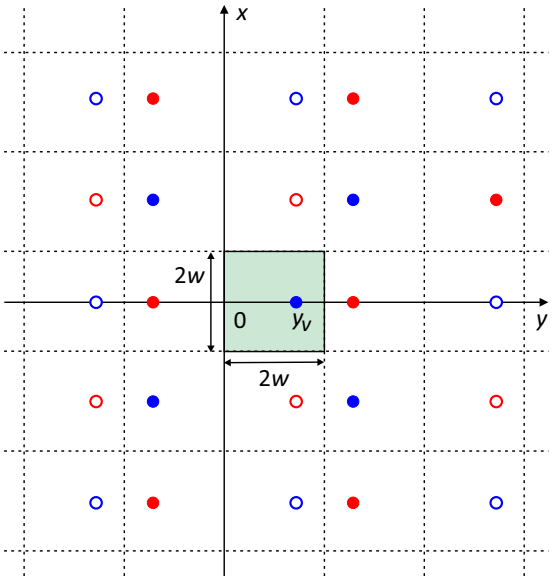

FIG. 10. The illustration of the image method which we use to calculate the magnetic field induced by the trapped vortex in the finite-size superconducting square. The blue circles correspond to the real vortex (when inside the square sample) and the image vortices, while the red circles show the image vortices with the opposite vorticity (antivortices). The filling of the circle indicates whether it makes a nonzero contribution into the attraction force F_{att} (filled circles) or not (nonfilled circles).

the attraction force on the y axis reads [53]

$$F_{\text{att}} = -t\Phi_0 \left.\frac{\partial H_z}{\partial y}\right|_{x=0,\, y=y_v}. \tag{37}$$

In the limit $t \ll \lambda$ the problem can be substantially simplified by neglecting the self-magnetic-fields generated by the vortex and the screening currents [54,55]. In this case the field H_z satisfies the Poisson equation which can be solved with the help of the electrostatic analogy [56,57]. According to this analogy, the field H_z plays the role of the electrostatic potential induced by the electrically charged wire with the linear charge density $Q = \epsilon_0\Phi_0/(\mu_0\lambda^2)$ and the boundary conditions at the sample edges can be fulfilled by introducing the set of the wire images which make the potential along the boundaries constant (in a full analogy with the well-known image method in electrostatics). Then the "potential" (magnetic field) at the point corresponding to the vortex center is the sum of the potentials created by all the "wire" images (see Fig. 10). At the same time, only the images whose distance from the real vortex changes with the variation of y_v make nonzero contribution into the attraction force (they are filled in Fig. 10), while the relative position of all other images with respect to the vortex does not depend on y_v and, thus, they can be excluded from further calculations. The coordinates of the contributing images have the form $(x_n; y_m)$ where $y_m = 2(2m+1)w - (y_v - w)$ and $x_n = 2(2n+1)w$ for the images with the charge Q and $x_n = 4nw$ for the ones with the opposite charge $-Q$; n and m are arbitrary integers $(-\infty < n,m < +\infty)$.

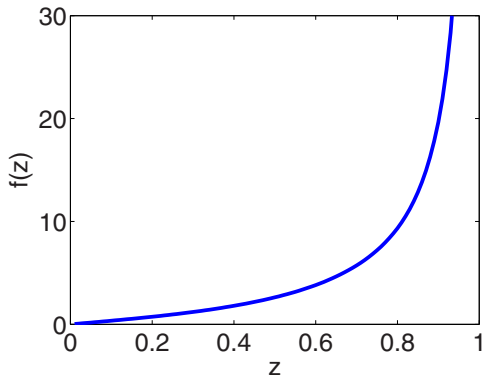

FIG. 11. The function $f(z)$ which defines the attractive force between the vortex and the boundaries of the square superconductor.

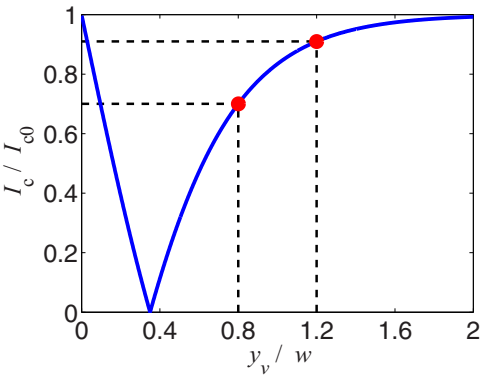

FIG. 12. The dependence of the critical current on the distance y_v between the vortex and the insulating layer (adopted from Ref. [33]). We take $x_v = 0$ assuming that the vortex is placed at the central line of the junction. The red points indicate the position of the pinning centers A and B. The critical current is normalized at the value $I_{c0} = 2j_c wt$.

Solving the Poisson equation we find that the magnetic field and the y projection of the resulting attracting force in the point corresponding to the vortex position read

$$H_z = C - \frac{1}{4\pi\epsilon_0}\sum_j 2Q_j \ln|\mathbf{r}_j - \mathbf{r}_v|, \tag{38}$$

$$F^y_{\rm att}(y_v) = -t\frac{\Phi_0}{4\pi\epsilon_0}\sum_j \frac{2Q_j(y_j - y_v)}{(y_j - y_v)^2 + x_j^2}, \tag{39}$$

where $\mathbf{r}_v = (0; y_v)$ is the vector of the vortex coordinates, $\mathbf{r}_j = (x_j; y_j)$ stays for the jth image, the summation is performed over all images which gives a nonzero contribution to the attracting force, and C is a certain constant which does not affect the attracting force.

Taking the sum in Eq. (39) we finally obtain

$$F^y_{\rm att}(y_v) = \frac{1}{4\pi\mu_0}\frac{t}{2w}\left(\frac{\Phi_0}{\lambda}\right)^2 f\left(\frac{y_v}{w} - 1\right). \tag{40}$$

The function $f(z)$ is defined as

$$f(z) = \sum_{n,m=-\infty}^{\infty} \frac{2(4m+1)p_n(z)}{\left[p_n^2(z) + (2m)^2\right]\left[p_n^2(z) + (2m+1)^2\right]}, \tag{41}$$

where $p_n(z) = 2n + 1 - z$. The plot of this function is shown in Fig. 11. For $z \ll 1$ the Taylor expansion gives $f(z) \approx 3.44z$ so that $F^y_{\rm att} \approx (1.72/4\pi\mu_0)(\Phi_0/\lambda)^2[(y_v - w)t/w^2]$.

To make the estimate we consider a Nb film with the critical temperature $T_c = 8$ K and the London penetration depth at zero temperature $\lambda(0) \sim 100$ nm [58]. For the sample of thickness $t = 5$ nm at temperature $T = 4.6$ K we find $\lambda_P \sim 4\ \mu$m and then the appropriate choice for the size of the square superconducting lead may be $2w \sim 3\ \mu$m. The pinning force f_p per unit length of the vortex can be estimated from the experimentally measured critical current density J_c of the isolated superconducting film due to the vortex depinning as $f_p = J_c\Phi_0$ [59]. Taking $J_c = 0.7 \times 10^6$ A/cm^2 which is relevant to the samples in Ref. [46] we find that $f_p \sim 10$ pN/μm. Thus, to neglect the vortex attraction to the sample boundaries one needs $F_{\rm att} \ll f_p t$, which is realized for $|y_v - w| \lesssim 0.2w \sim 300$ nm.

The insulating film of the Josephson junction should be chosen in a way that the Josephson energy $\varepsilon_J \times 2w$ exceeds the system temperature T. This requirement is satisfied provided the critical current density of the junction is $j_c \gtrsim 2\pi T/(2wt\Phi_0) \approx 1.2$ kA/cm^2 which is an achievable value for the Josephson systems.

The distance Δy between the artificial pinning centers A and B should be chosen large enough to guarantee the reliable displacement of the vortex when applying the laser beam and, at the same time, small enough to optimize the switching time and avoid the vortex interaction with the sample boundaries (we need $\Delta y < 2|y_v - w|$). In experiment the vortex has been successfully moved at the distances $\sim 1\ \mu$m comparable to the laser beam radius $r_0 \sim 0.4\ \mu$m [46], so it is reasonable to choose the position of the pinning centers $y_A = 0.8w$ and $y_B = 1.2w$ so that the distance between them is $\Delta y \sim 600$ nm.

The pinning force estimated above allows us to determine the optimal parameters for the focused laser beam controlling the vortex position. The thermal force acting on the vortex from the beam is proportional to the temperature gradient $(\nabla T)_v$ at the point of the vortex, and the depinning occurs when

$$\Phi_0\frac{\partial H_{c1}}{\partial T}(\nabla T)_v \geqslant f_p. \tag{42}$$

For $f_p \sim 10$ pN/μm one finds that the condition (42) is satisfied for $(\nabla T)_v \sim 2$ K/μm. Modeling the temperature profile in the superconductor under the influence of the laser beam in the spirit of Ref. [46] we obtain that to provoke the vortex motion at a distance $\Delta y \sim 600$ nm from the initial position one needs a beam of the power $W \sim 500\ \mu$W (we took the absorbtion coefficient equal to 50%).

The optically controlled vortex motion between the points $y = (1 \pm 0.2)w$ should produce the variation of the Josephson critical current which exceeds 15%, namely, from $0.9I_c$ to $0.73I_c$ (see Fig. 12). This change may be easily detected on transport experiments allowing us to realize the effective read-out procedure in the described memory cell. The numerical analysis of the heat transport equation with the parameters relevant to Nb and the substrates used in Ref. [46] shows that the characteristic switching time between the different vortex positions in the memory cell is on the order of $\tau \sim 10$ ps which gives the energy per operation $E \sim 3 \times 10^{-15}$ J.

Thus, the Josephson junction with the embedded vortex is a promising system which can serve as a basic optically controlled memory cell working at the subterahertz frequencies.

V. CONCLUSION

To sum up, we demonstrate that an Abrikosov vortex pinned near the Josephson junction produces the anomalous Josephson effect revealing itself through the emergence of the arbitrary Josephson phase in the ground state. Changing the vortex position along the specific trajectories, e.g., with the help of the focused laser beam, one can produce controllable phase transitions between the states with different Josephson phase values. In particular, for planar junctions of the thickness $t \gtrsim \lambda$ depending on the vortex trajectory such phase transitions can be of the first or second type which corresponds to the steplike switching between the zero and π states or the continuous phase changing through the φ_0-junction formation, respectively. For the thin junctions with $t \lesssim \lambda$ the vortex-induced 0-π transitions seem to be a promising tool for the design of the ultrafast optically controlled memory cells for the cryogenic electronics where the information is encoded in the position of the vortex, the writing is performed by the laser, and the readout is realized on the basis of the Josephson current measurement. Note that in spite of the assumptions about the ratio t/λ which allow us to simplify the analytical analysis in different limiting cases all discovered phenomena should be generic and remain qualitatively the same for arbitrary relations between t and λ. Thus, we hope that our results can be directly verified in existing experimental setups [46] and will stimulate future progress in the domain of optofluxonics.

ACKNOWLEDGMENTS

This work was partially supported by the French ANR projects "SUPERTRONICS" and "Optofluxonics," the Russian Foundation for Basic Research and EU COST Action CA16218. E.G. and S.M. thank the University of Bordeaux for financial support and hospitality. A.B. wish to thank the *Leverhulme Trust* for supporting his stay in Cambridge University. E.G. acknowledges support by the Deutsche Forschungsgemeinschaft (DFG) via Project No. GO-1106/5.

[1] A. I. Buzdin, Rev. Mod. Phys. **77**, 935 (2005).
[2] M. Eschrig, Rep. Prog. Phys. **78**, 104501 (2015).
[3] A. Bauer, J. Bentner, M. Aprili, M. L. Della-Rocca, M. Reinwald, W. Wegscheider, and C. Strunk, Phys. Rev. Lett. **92**, 217001 (2004).
[4] A. I. Buzdin, Phys. Rev. B **72**, 100501 (2005).
[5] A. K. Feofanov, V. A. Oboznov, V. V. Bol'ginov, J. Lisenfeld, S. Poletto, V. V. Ryazanov, A. N. Rossolenko, M. Khabipov, D. Balashov, A. B. Zorin, P. N. Dmitriev, V. P. Koshelets, and A. V. Ustinov, Nat. Phys. **6**, 593 (2010).
[6] T. Ortlepp, Ariando, O. Mielke, C. J. M. Verwijs, K. F. K. Foo, H. Rogalla, F. H. Uhlmann, and H. Hilgenkamp, Science **312**, 1495 (2006).
[7] I. I. Soloviev, N. V. Klenov, S. V. Bakurskiy, V. V. Bol'ginov, V. V. Ryazanov, M. Yu. Kupriyanov, and A. A. Golubov, Appl. Phys. Lett. **105**, 242601 (2014).
[8] A. Mukhanov, IEEE Trans. Appl. Supercond. **21**, 760 (2011).
[9] A. I. Buzdin, L. Bulaevskii, and S. V. Panyukov, Sov. Phys. JETP **35**, 178 (1982).
[10] V. V. Ryazanov, V. A. Oboznov, A. Y. Rusanov, A. V. Veretennikov, A. A. Golubov, and J. Aarts, Phys. Rev. Lett. **86**, 2427 (2001).
[11] V. A. Oboznov, V. V. Bol'ginov, A. K. Feofanov, V. V. Ryazanov, and A. I. Buzdin, Phys. Rev. Lett. **96**, 197003 (2006).
[12] C. Gürlich, S. Scharinger, M. Weides, H. Kohlstedt, R. G. Mints, E. Goldobin, D. Koelle, and R. Kleiner, Phys. Rev. B **81**, 094502 (2010).
[13] H. Sickinger, A. Lipman, M. Weides, R. G. Mints, H. Kohlstedt, D. Koelle, R. Kleiner, and E. Goldobin, Phys. Rev. Lett. **109**, 107002 (2012).
[14] T. Gaber, E. Goldobin, A. Sterck, R. Kleiner, D. Koelle, M. Siegel, and M. Neuhaus, Phys. Rev. B **72**, 054522 (2005).
[15] A. V. Ustinov, Appl. Phys. Lett. **80**, 3153 (2002).
[16] E. Goldobin, S. Mironov, A. Buzdin, R. G. Mints, D. Koelle, and R. Kleiner, Phys. Rev. B **93**, 134514 (2016).
[17] A. Buzdin, Phys. Rev. Lett. **101**, 107005 (2008).
[18] S. V. Mironov, A. S. Mel'nikov, and A. I. Buzdin, Phys. Rev. Lett. **114**, 227001 (2015).
[19] F. Dolcini, M. Houzet, and J. S. Meyer, Phys. Rev. B **92**, 035428 (2015).
[20] D. B. Szombati, S. Nadj-Perge, D. Car, S. R. Plissard, E. P. A. M. Bakkers, and L. P. Kouwenhoven, Nat. Phys. **12**, 568 (2016).
[21] M. Eschrig, A. Cottet, W. Belzig, and J. Linder, New J. Phys. **17**, 083037 (2015).
[22] S. Mironov and A. Buzdin, Phys. Rev. B **92**, 184506 (2015).
[23] A. Moor, A. F. Volkov, and K. B. Efetov, Phys. Rev. B **92**, 180506(R) (2015).
[24] A. V. Veretennikov, V. V. Ryazanov, V. A. Oboznov, A. Y. Rusanov, V. A. Larkin, and J. Aarts, Phys. B (Amsterdam, Neth.) **284-288**, 495 (2000).
[25] V. V. Ryazanov, V. A. Oboznov, A. S. Prokofiev, V. V. Bolginov, and A. K. Feofanov, J. Low Temp. Phys. **136**, 385 (2004).
[26] Y. Blum, A. Tsukernik, M. Karpovski, and A. Palevski, Phys. Rev. Lett. **89**, 187004 (2002).
[27] C. Li, A. Kasumov, A. Murani, S. Sengupta, F. Fortuna, K. Napolskii, D. Koshkodaev, G. Tsirlina, Y. Kasumov, I. Khodos, R. Deblock, M. Ferrier, S. Guéron, and H. Bouchiat, Phys. Rev. B **90**, 245427 (2014).
[28] K. Buckenmaier, T. Gaber, M. Siegel, D. Koelle, R. Kleiner, and E. Goldobin, Phys. Rev. Lett. **98**, 117006 (2007).
[29] A. Dewes, T. Gaber, D. Koelle, R. Kleiner, and E. Goldobin, Phys. Rev. Lett. **101**, 247001 (2008).
[30] L. G. Aslamazov and E. V. Gurovich, Pis'ma Zh. Eksp. Teor. Fiz. **40**, 22 (1984).
[31] M. V. Fistul and G. F. Giuliani, Phys. Rev. B **58**, 9343 (1998).
[32] T. Golod, A. Rydh, and V. M. Krasnov, Phys. Rev. Lett. **104**, 227003 (2010).
[33] J. R. Clem, Phys. Rev. B **84**, 134502 (2011).
[34] T. Golod, A. Iovan, and V. M. Krasnov, Nat. Commun. **6**, 8628 (2015).

[35] N. Uchida, K. Enpuku, Y. Matsugaki, S. Tomita, and F. Irie, J. Appl. Phys. **54**, 5287 (1983).
[36] S. L. Miller, K. R. Biagi, J. R. Clem, and D. K. Finnemore, Phys. Rev. B **31**, 2684 (1985).
[37] A. A. Golubov and M. Yu. Kupriyanov, Zh. Eksp. Teor. Fiz. **92**, 1512 (1987).
[38] A. A. Golubov and M. Yu. Kupriyanov, J. Low Temp. Phys. **70**, 83 (1988).
[39] V. N. Gubankov, M. P. Lisitskii, I. L. Serpuchenko, F. N. Sklokin, and M. V. Fistul', Supercond. Sci. Technol. **5**, 168 (1992).
[40] A. A. Golubov and A. V. Ustinov, Phys. Lett. A **162**, 409 (1992).
[41] A. V. Ustinov, T. Doderer, B. Mayer, R. P. Huebener, A. A. Golubov, and V. A. Oboznov, Phys. Rev. B **47**, 944 (1993).
[42] A. V. Samokhvalov, Phys. Rev. B **80**, 134513 (2009).
[43] E. W. J. Straver, J. E. Hoffman, O. M. Auslaender, D. Rugar, and K. A. Moler, Appl. Phys. Lett. **93**, 172514 (2008).
[44] O. M. Auslaender, L. Luan, E. W. J. Straver, J. E. Hoffman, N. C. Koshnick, E. Zeldov, D. A. Bonn, R. Liang, W. N. Hardy, and K. A. Moler, Nat. Phys. **5**, 35 (2009).
[45] J.-Y. Ge, V. N. Gladilin, J. Tempere, C. Xue, J. T. Devreese, J. Van de Vondel, Y. Zhou, and V. V. Moshchalkov, Nat. Commun. **7**, 13880 (2016).
[46] I. S. Veshchunov, W. Magrini, S. V. Mironov, A. G. Godin, J.-B. Trebbia, A. I. Buzdin, Ph. Tamarat, and B. Lounis, Nat. Commun. **7**, 12801 (2016).
[47] V. G. Kogan and R. G. Mints, Phys. C (Amsterdam, Neth.) **502**, 58 (2014).
[48] R. A. Ferrell and R. E. Prange, Phys. Rev. Lett. **10**, 479 (1963).
[49] F. London and H. London, Proc. R. Soc. A **149**, 71 (1935).
[50] V. G. Kogan and R. G. Mints, Phys. Rev. B **89**, 014516 (2014).
[51] G. R. Berdiyorov, M. V. Milosevic, L. Covaci, and F. M. Peeters, Phys. Rev. Lett. **107**, 177008 (2011).
[52] J. Pearl, Appl. Phys. Lett. **5**, 65 (1964).
[53] P. G. de Gennes, *Superconductivity of Metals and Alloys* (Westview Press, 1999).
[54] M. Moshe, V. G. Kogan, and R. G. Mints, Phys. Rev. B **78**, 020510(R) (2008).
[55] J. R. Clem, Phys. Rev. B **81**, 144515 (2010).
[56] A. Buzdin and D. Feinberg, Phys. C (Amsterdam, Neth.) **235-240**, 2755 (1994).
[57] A. Buzdin and D. Feinberg, Phys. C (Amsterdam, Neth.) **256**, 303 (1996).
[58] T. R. Lemberger, I. Hetel, J. W. Knepper, and F. Y. Yang, Phys. Rev. B **76**, 094515 (2007).
[59] D. Saint-James, G. Sarma, and E. J. Thomas, *Type II Superconductivity* (Pergamon Press, Oxford, 1969).